The University of Nottingham
UNITED KINGDOM · CHINA · MALAYSIA

Sagonas, Christos and Antonakos, Epameinondas and Tzimiropoulos, Georgios and Zafeiriou, Stefanos and Pantic, Maja (2016) 300 faces in-the-wild challenge: database and results. Image and Vision Computing . ISSN 0262-8856

Access from the University of Nottingham repository:
http://eprints.nottingham.ac.uk/31549/1/tzimiroIVC16.pdf

Copyright and reuse:

The Nottingham ePrints service makes this work by researchers of the University of Nottingham available open access under the following conditions.

This article is made available under the Creative Commons Attribution Non-commercial No Derivatives licence and may be reused according to the conditions of the licence. For more details see: http://creativecommons.org/licenses/by-nc-nd/2.5/

A note on versions:

The version presented here may differ from the published version or from the version of record. If you wish to cite this item you are advised to consult the publisher's version. Please see the repository url above for details on accessing the published version and note that access may require a subscription.

For more information, please contact eprints@nottingham.ac.uk

Accepted Manuscript

300 faces In-the-wild challenge: Database and results

Christos Sagonas, Epameinondas Antonakos, Georgios Tzimiropoulos, Stefanos Zafeiriou, Maja Pantic

PII: S0262-8856(16)00014-7
DOI: doi: 10.1016/j.imavis.2016.01.002
Reference: IMAVIS 3455

To appear in: *Image and Vision Computing*

Received date: 19 March 2015
Revised date: 2 October 2015
Accepted date: 4 January 2016

Please cite this article as: Christos Sagonas, Epameinondas Antonakos, Georgios Tzimiropoulos, Stefanos Zafeiriou, Maja Pantic, 300 faces In-the-wild challenge: Database and results, *Image and Vision Computing* (2016), doi: 10.1016/j.imavis.2016.01.002

This is a PDF file of an unedited manuscript that has been accepted for publication. As a service to our customers we are providing this early version of the manuscript. The manuscript will undergo copyediting, typesetting, and review of the resulting proof before it is published in its final form. Please note that during the production process errors may be discovered which could affect the content, and all legal disclaimers that apply to the journal pertain.

ACCEPTED MANUSCRIPT

300 Faces In-The-Wild Challenge: Database and Results

Christos Sagonas[a,*], Epameinondas Antonakos[a,**], Georgios Tzimiropoulos[b], Stefanos Zafeiriou[a], Maja Pantic[a,c]

[a] *Imperial College London, Department of Computing, London, U.K.*
[b] *University of Nottingham, School of Computer Science, Nottingham, U.K.*
[c] *Faculty of Electrical Engineering, Mathematics, and Computer Science, University of Twente, The Netherlands*

Abstract

Computer Vision has recently witnessed great research advance towards automatic facial points detection. Numerous methodologies have been proposed during the last few years that achieve accurate and efficient performance. However, fair comparison between these methodologies is infeasible mainly due to two issues. (a) Most existing databases, captured under both constrained and unconstrained (in-the-wild) conditions have been annotated using different mark-ups and, in most cases, the accuracy of the annotations is low. (b) Most published works report experimental results using different training/testing sets, different error metrics and, of course, landmark points with semantically different locations. In this paper, we aim to overcome the aforementioned problems by (a) proposing a semi-automatic annotation technique that was employed to re-annotate most existing facial databases under a unified protocol, and (b) presenting the 300 Faces In-The-Wild Challenge (300-W), the first facial landmark localization challenge that was organized twice, in 2013 and 2015. To the best of our knowledge, this is the first effort towards a unified annotation scheme of massive databases and a fair experimental comparison of existing facial landmark localization systems. The images and annotations of the new testing database that was used in the 300-W challenge are available from http://ibug.doc.ic.ac.uk/resources/facial-point-annotations/.

Keywords: facial landmark localization, challenge, semi-automatic annotation tool, facial database

*Corresponding author. E-mail: mailto:c.sagonas@imperial.ac.uk c.sagonas@imperial.ac.uk

**The contribution of the first two authors on writing this paper is equal, with Christos Sagonas being the main responsible for the implementation and execution of various steps needed to run 300-W successfully including data annotation, annotation tools development, and running the experiments.

ACCEPTED MANUSCRIPT

1. Introduction

During the last decades we notice a wealth of scientific research in computer vision for the problem of facial landmark points localization using visual deformable models. The main reason behind this are the countless applications that the problem has in human-computer interaction and facial expressions recognition. Numerous methodologies have been proposed that are shown to achieve great accuracy and efficiency. They can be roughly divided into two categories: *generative* and *discriminative*. The generative techniques, which aim to find the parameters that maximize the probability of the test image being generated by the model, include Active Appearance Models (AAMs) [1, 2], their improved extensions [3, 4, 5, 6, 7, 8, 9, 10] and Pictorial Structures [11, 12]. The discriminative techniques can be further divided to those that use discriminative response map functions, such as Active Shape Models (ASMs) [13], Constrained Local Models (CLMs) [14, 15, 16] and Deformable Part Models (DPMs) [17], those that learn a cascade of regression functions, such as Supervised Descent Method (SDM) [18] and others [19, 20, 21], and, finally, those that employ random forests [22, 23].

Arguably, the main reason why many researchers of the field focus on the problem of face alignment is the plethora of publicly available annotated facial databases. These databases can be separated in two major categories: (a) those captured under *controlled conditions*, e.g. Multi-PIE [24], XM2VTS [25], FRGC-V2 [26], AR [27], and those captured under totally *unconstrained conditions* (in-the-wild), e.g. LFPW [28], HELEN [29], AFW [17], AFLW [30], IBUG [31]. All of them cover large variations, including different subjects, pose, illumination, expressions and occlusions. However, for most of them, the provided annotations appear to have several limitations. Specifically:

- The majority of them provide annotations for a relatively small subset of images.
- The annotation mark-up of each database consists of different number of landmark points with semantically different locations.
- The accuracy of the provided annotations in some cases is limited.

The above issues are due to the fact that manual annotation of large databases is a highly time consuming procedure that requires enormous workload and a trained expert. Moreover, factors like fatigue and lack of concentration are among the reasons why, in some cases, annotations are inaccurate. This highlights the need of creating a (semi-) automatic annotation tool.

Furthermore, by going through the published works of the last years, one can easily notice that the setup of the experiments is not always correct. Researchers employ different databases, experimental protocols and performance metrics, which lead to unfair comparisons between existing methods. Some characteristic such examples are the following:

ACCEPTED MANUSCRIPT

- Authors compare their techniques against other state-of-the-art, but they do so by using, in many cases, completely different databases for training compared to the ones that the other methods were originally trained on.
- Authors compare their techniques on specific databases by replicating the originally presented curves and not the experiment.
- In some cases, authors report results on databases from which only a part can be used by the community, as some of the training/testing images are no longer publicly available.

Evidence shows that there is a lack of access to properly evaluate existing methods. Even though there exist open-source implementations of various state-of-the-art techniques (the most characteristic example is Menpo [32]), researchers still do not employ a unified benchmark. Since we are unaware of the achieved performances, it is impossible to investigate how far we are from attaining satisfactory performance. Therefore, a new evaluation needs to be carried out, using a unified experimental protocol.

Various methods have been proposed in the literature for the task of landmark localization under semi-supervised or weakly-supervised settings [33, 34, 35, 36]. However, there are two major limitations of these methods. Firstly, most existing methodologies require additional information regarding the input images. Specifically, [33] employs the corresponding facial mask for each of the training images. The purpose of these masks is to indicate which pixels belong to the facial area and the only way to produce them is by manually annotating each image. In [34], the training procedure requires as input the orientation of each face depicted in the training images. Secondly, and most importantly, existing methods, such as [35] and [36], have only been applied on images that are captured under controlled conditions. The aforementioned issues, make the existing methods incapable for the task of semi-automatic annotation of large databases with in-the-wild images (most of the images are downloaded from the web with simple search queries), which is a much more challenging task.

Semi-automatic annotation systems can greatly benefit from the employment of generative models. Let us assume that we have cohorts of both annotated and non-annotated images. By training a generative model, such as AAMs, using the annotated images, we get a parametric model that describes the facial shape and appearance. Most importantly, the model can naturally generate novel instances of human face, by combining the shape and appearance variance of the training annotated images. This could enable the generation of instances that resemble accurately with the shape and appearance of the subjects in the non-annotated images. For instance, by training a model using images from one view (e.g. pose 15°) with neutral expression and images from another view (e.g. pose 0°) with a non-neutral expression, one can fit the model to an instance that has the non-neutral expression with pose of 15°. However, the fitting procedure of a generative deformable model is a very tedious task, mainly because many of the models that have been proposed till now do not generalize well to unseen images. One of the AAM variants that has satisfactory generalization properties

ACCEPTED MANUSCRIPT

is Active Orientation Models (AOMs) [3, 4]. AOMs are shown to be robust in cases with large variations, such as occlusions, extreme illumination etc., and outperform discriminative methodologies, such as CLMs [15], DPMs [17] and SDM [18].

Motivated by the success of AOMs in generic face alignment, we propose, in this paper, a semi-automatic technique for annotating in a time efficient manner massive facial databases. We employed the proposed tool to re-annotate all the widely used databases, i.e. Multi-PIE [24], XM2VTS [25], FRGC-V2 [26], AR [27], LFPW [28], HELEN [29] and AFW [17]. The resulting annotations[1] are, in many cases, more accurate than the original ones and employ a unified mark-up scheme, thus overcome the limitations explained above.

Furthermore, in order to offer to the research community the ability to carry out rational comparisons between existing and future proposed methods, we organized two versions of the 300 Faces In-The-Wild Challenge (300-W), the first automatic facial landmark detection in-the-wild challenge. The first challenge[2] was organized in 2013 in conjunction with the IEEE International Conference on Computer Vision (ICCV'13) [31]. The second conduct[3] of the challenge was completed in the beginning of 2015. In both conducts, the training set consisted of the XM2VTS, FRGC-V2, LFPW, HELEN, AFW and IBUG databases that were annotated using the proposed semi-automatic procedure. Additionally, we collected and annotated a new challenging in-the-wild database that was used for testing[4]. The 300-W database consists of 300 *Indoor* and 300 *Outdoor* images downloaded from the web, thus captured under totally unconstrained conditions. The performance of the submitted methods was evaluated using the same fitting accuracy metric. The major difference between the two conducts of the challenge is that in the first version we provided the bounding boxes of the testing images to be used as initializations, while in the second version the participants were required to submit systems that performed both face detection and alignment. Additionally, contrary to the first version, in the second one the submitted methods were also compared with respect to their computational costs.

The contribution of this paper can be summarized as follows:

1. We propose a semi-automatic methodology for facial landmark points annotation. The proposed tool was employed in order to re-annotate large facial databases and overcome the major issues of the original annotations.
2. We present and analyse the results of the 300 Faces In-The-Wild Challenge (300-W), the first facial landmark localization challenge, that was

[1]The annotations of XM2VTS, FRGC-V2, LFPW, HELEN, AFW and IBUG are publicly available from http://ibug.doc.ic.ac.uk/resources/facial-point-annotations/.

[2]The first conduct of the 300-W Challenge (2013) is available in http://ibug.doc.ic.ac.uk/resources/300-W/

[3]The second conduct of the 300-W Challenge (2015) is available in http://ibug.doc.ic.ac.uk/resources/300-W_IMAVIS/

[4]The 300-W database is publicly available from http://ibug.doc.ic.ac.uk/resources/facial-point-annotations/. We provide the original and cropped, as well as the bounding boxes.

ACCEPTED MANUSCRIPT

conducted twice, in 2013 and 2015. The challenge is the first attempt towards a fair comparison of existing methods using a unified experimental protocol.

3. We make the very challenging 300-W dataset publicly available to the research community. It was employed as testing set in both conducts of the 300-W competition.

The rest of the paper is organized as follows: Section 2 gives an overview of the available facial databases. Section 3 presents the proposed semi-automatic methodology for facial landmark points annotations along with the re-annotated databases. The 300-W challenge and the results are described in details in Section 4. Finally, Section 5 summarizes the results of this work and draws conclusions.

2. Overview of Existing Facial Databases

There exist numerous facial databases which partially justifies the research advances for the task of face alignment. These databases exhibit large variations in resolution, image quality, identity, head pose, facial expression, lighting conditions and partial occlusion. As mentioned before, the existing databases can be split in two major categories. The first category includes databases that are captured under *controlled conditions*, normally within special indoor laboratories/studios in which the camera position and the lighting source and intensity can be controlled. In most of these databases, each subject is asked to perform a posed facial expression, thus we find more than one images per subject. The most popular such databases are Multi-PIE [24] (used for face recognition, expressions recognition, landmark points localization), FRGC-V2 [26] (used for face recognition), XM2VTS [25] and AR [27] (both used for face recognition and landmark points localization). The facial databases of the second major category consist of images that are captured under totally *unconstrained conditions (in-the-wild)*. In most cases, these images are downloaded from the web by making face-related queries to various search engines. The most notable databases of this category are LFPW [28], HELEN [29], AFW [17], AFLW [30] and IBUG [31] (all used for facial landmark points localization).

The majority of the aforementioned databases provide annotations for a relatively small subset of images. Moreover, as shown in Fig. 1, they all have different annotation schemes between them, leading in different number of points with semantically different locations. There are also cases in which the accuracy of the provided annotations is limited. Sections 2.1, 2.2 and Table 1 provide an overview of the characteristics of all the commonly-used existing databases.

2.1. Facial databases under controlled conditions

Multi-PIE: The CMU Multi Pose Illumination, and Expression (Multi-PIE) Database [24] contains around 750000 images of 337 subjects captured under laboratory conditions in four different sessions. For each subject, there are available images for 15 different poses, 19 illumination conditions and 6

ACCEPTED MANUSCRIPT

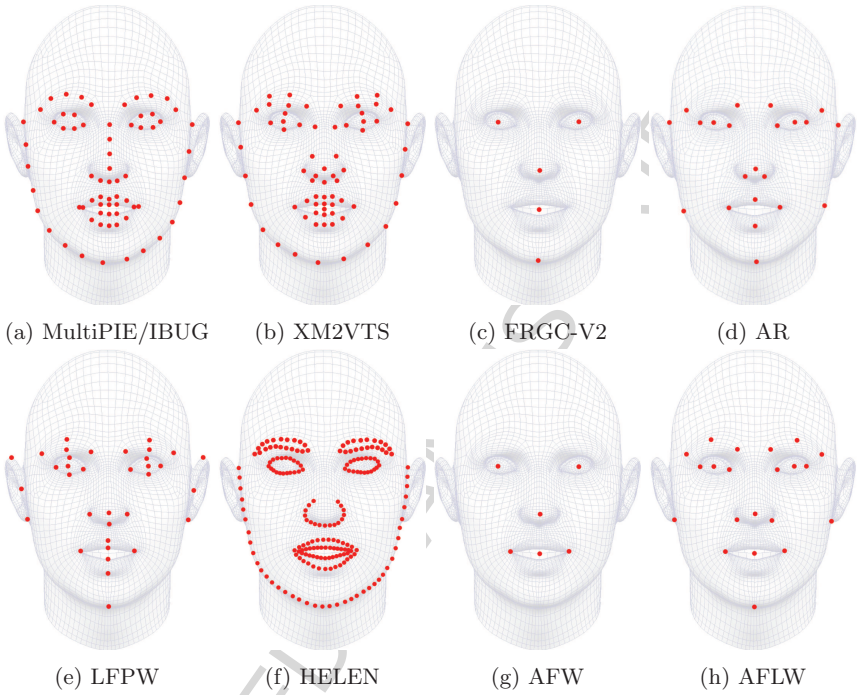

(a) MultiPIE/IBUG (b) XM2VTS (c) FRGC-V2 (d) AR

(e) LFPW (f) HELEN (g) AFW (h) AFLW

Figure 1: Landmarks configurations of existing databases. Note they all have different number of landmark points with semantically different locations.

different expressions (neutral, scream, smile, squint, surprise, disgust). The accompanying facial landmark annotations consist of a set of 68 points (Fig. 1a) for images in the range $[-45°, 45°]$.

XM2VTS: The Extended Multi Modal Verification for Teleservices and Security applications (XM2VTS) [25] database contains 2360 frontal images of 295 different subjects. Each subject has two available images for each of the four different sessions. All subjects are captured under the same illumination conditions and in the majority of images the subject has neutral expression. Facial landmark annotations of the whole database are available, where 68 points are provided for each image (Fig. 1b). However, the accuracy of the annotations in some cases is limited and the locations of the provided points do not correspond to ones of Multi-PIE.

FRGC-V2: The Face Recognition Grand Challenge Version 2.0 (FRGC-V2) database [26] consists of 4950 facial images of 466 different subjects. Each subject session consists of images captured under well-controlled conditions (i.e., uniform illumination, high resolution) and images captured under fairly uncontrolled conditions such as non-uniform illumination and poor quality. The provided annotations consist of 5 landmark points (Fig. 1c) only.

AR: The AR Face Database [27] contains over 4000 images corresponding to

ACCEPTED MANUSCRIPT

Database	*conditions*	*# faces*	*# subjects*	*# points*	*pose*
Multi-PIE	controlled	~ 750000	337	68	$[-45°, 45°]$
XM2VTS		2360	295	68	$0°$
FRGC-V2		4950	466	5	$0°$
AR		~ 4000	126	22	$0°$
LFPW	in-the-wild	1035	–	35	$[-45°, 45°]$
HELEN		2330		194	
AFW		468		6	
AFLW		25993		21	
IBUG		135		68	

Table 1: Overview of the characteristics of existing facial databases.

126 subjects (70 male, 56 female). The images were captured in two sessions per subject and have frontal pose with variations in facial expressions, illumination conditions and occlusions (sunglasses and scarf). The images are annotated using 22 landmark points (Fig. 1d).

2.2. Facial databases under in-the-wild conditions

LFPW: The Labeled Face Parts in the Wild (LFPW) database [28] contains 1287 images downloaded from the internet (i.e., google.com, flickr.com, and yahoo.com). This database provides only the web URLs and not the actual images. We were therefore able to download only a subset of 811 out of 1100 training images and 224 out of 300 test images, due to broken links. These images contain large variations in pose, expressions, illumination conditions and occlusions. The provided ground truth annotations consist of 35 landmark points (Fig. 1e) and low accuracy is observed in several cases.

HELEN: The HELEN [29] database consists of 2330 images downloaded from flickr.com web service, that contain a broad range of appearance variation, including pose, illumination, expression, occlusion and identity. The approximate face size of each image is 500×500 pixels. The provided annotations are very detailed and contain 194 landmark points (Fig.1f), but the accuracy is limited.

AFW: The Annotated Faces in-the-wild (AFW) [17] database consists of 250 images with 468 faces, that is, more than one faces are annotated in each image. The images exhibit similar variations with those in the aforementioned in-the-wild databases. Facial landmark annotations are available for the whole database, but the annotation mark-up consists of only 6 points (Fig. 1g).

AFLW: The Annotated Facial Landmarks in the Wild (AFLW) [30] database consists of 25993 images gathered from Flickr, exhibiting a large variety in appearance (e.g., pose, expression, ethnicity, age, gender) as well as general imaging and environmental conditions. However, the employed annotation scheme only includes 21 landmark points (Fig. 1h).

IBUG: The IBUG database was released as part of the first version of the 300-W challenge [31]. It consists of 135 images downloaded from the web,

ACCEPTED MANUSCRIPT

with large variations in expression, illumination and pose. The provided facial landmark annotations are produced by employing the annotation scheme of Multi-PIE (Fig. 1a).

3. Semi-Automatic Annotation Tool

In this section, we propose a technique for semi-automatic annotation of large databases, which takes advantage of the good generalization properties of AOMs [3, 4].

3.1. Active Orientation Models

AOMs is a variant of AAMs [2]. Similar to AAMs, they consist of parametric statistical shape and appearance models, and a deformation model. However, the difference is that AOMs employ kernel PCA based on a similarity criterion that is robust to outliers. Specifically, the appearance model of AOMs consists of the principal components of image gradient orientations [37], which makes them generalize well to unseen face instances.

Let us assume that we have a set of D training images, $\{\mathbf{I}_1, \ldots, \mathbf{I}_D\}$, annotated with N landmark points that represent the ground truth shape of each image. A shape instance is defined as the $2N \times 1$ vector $\mathbf{s} = [x_1, y_1, \ldots, x_N, y_N]^T$, where (x_i, y_i) are the coordinates of the i-th fiducial point. The *shape model* is constructed by first aligning all training shapes using Generalized Procrustes Analysis in order to remove global similarity transformations and then applying Principal Component Analysis (PCA) on the aligned shapes to retrieve:

$$\left\{\bar{\mathbf{s}}, \mathbf{U}_S \in \mathbb{R}^{2N \times N_S}\right\}, \tag{1}$$

where $\bar{\mathbf{s}}$ is the mean shape and $\mathbf{U}_S$ consists of the first N_S eigenvectors with the highest variance. A novel shape instance can be generated as:

$$\mathbf{s} = \bar{\mathbf{s}} + \mathbf{U}_S \mathbf{p}, \tag{2}$$

where $\mathbf{p} = [p_1, \ldots, p_{N_S}]^T$ denotes the $N_S \times 1$ vector of shape parameters. The *deformation model* consists of a warp function, denoted as $\mathcal{W}(\mathbf{p})$, which maps all the pixels that belong into a shape instance generated from Eq. 2 with parameters $\mathbf{p}$ to their corresponding locations in the mean shape $\bar{\mathbf{s}}$. We employ the Piecewise Affine Warp, which evaluates the mapping using the barycentric coordinates of the triangles extracted with Delaunay triangulation.

The appearance model of an AOM is based on normalized gradients [37]. Let us denote an image in vectorial form as $\mathbf{i}$ with size $L \times 1$, thus L is the number of pixels. Moreover, we denote $\mathbf{g}_x$, $\mathbf{g}_y$ to be the image gradients and $\boldsymbol{\phi} = \arctan(\mathbf{g}_x / \mathbf{g}_y)$ the corresponding gradient orientation vector. The normalized gradients extraction function is defined as:

$$\mathcal{Z}(\mathbf{i}) = \frac{1}{\sqrt{L}} [\cos \boldsymbol{\phi}^T, \sin \boldsymbol{\phi}^T]^T, \tag{3}$$

ACCEPTED MANUSCRIPT

where $\cos\boldsymbol{\phi} = [\cos\boldsymbol{\phi}(1), \ldots, \cos\boldsymbol{\phi}(L)]^T$ and $\sin\boldsymbol{\phi} = [\sin\boldsymbol{\phi}(1), \ldots, \sin\boldsymbol{\phi}(L)]^T$. By employing the deformation model, we can define the shape-free normalized gradients of an image $\mathbf{i}$ as the $2L_A \times 1$ vector:

$$\mathbf{z}(\mathbf{p}) \equiv \mathcal{Z}(\mathbf{i}(\mathcal{W}(\mathbf{p}))), \tag{4}$$

where L_Z is the number of pixels that belong to the mean shape $\bar{\mathbf{s}}$, which has the role of the reference shape. By applying PCA on the warped normalized gradients of the training images, i.e. $\{\mathbf{z}_1, \ldots, \mathbf{z}_D\}$, we construct an *appearance model* of the form:

$$\mathbf{U}_Z \in \mathbb{R}^{2L_Z \times N_Z}, \tag{5}$$

where $\mathbf{U}_Z$ stores the first N_Z eigenvectors with the highest variance. Note that in order to preserve the robust property of the normalized gradients kernel, we don't subtract the mean appearance vector from the training set, so it ends up as the first eigenvector. A novel appearance instance can be generated as:

$$\mathbf{z} = \mathbf{U}_Z\mathbf{c}, \tag{6}$$

where $\mathbf{c} = [c_1, \ldots, c_{N_Z}]^T$ denotes the $N_Z \times 1$ vector of appearance parameters.

Given a testing image $\mathbf{t}$ in vectorized form and the trained shape, appearance and deformation models, the fitting procedure aims to minimize:

$$\arg\min_{\mathbf{p},\mathbf{c}} \|\mathbf{z}(\mathbf{p}) - \mathbf{U}_Z\mathbf{c}\|^2, \tag{7}$$

where $\mathbf{z}(\mathbf{p})$ denotes the normalized gradients of $\mathbf{t}$, as defined in Eq. 4. This optimization can be efficiently solved in an inverse compositional alternating manner, as shown in [3, 4, 38].

3.2. Method

The main idea behind the proposed tool is to take advantage of the generalization qualities of AOMs by building a model using annotated images with various poses and expressions and generate the annotations on images with different poses and expressions. Specifically, let us denote a database that consists of N_{subj} subjects as $\mathcal{DB}$. We assume that for each subject, images with different expressions $\{E_j\},\ j \in \{1, 2, \ldots, N_{exp}\}$, and poses $\{P_k\},\ k \in \{1, 2, \ldots, N_{pos}\}$ are available. Let $\mathcal{V}$ be a subset of annotated images and $\mathcal{Q}$ a subset of non-annotated images of $\mathcal{DB}$. The goal of our tool is to **(1)** generate annotations for the subjects in $\mathcal{Q}$ which appear in $\mathcal{V}$ with different expressions and poses, and **(2)** generate annotations for the subjects of $\mathcal{Q}$ that are not included in $\mathcal{V}$. For example, in Multi-PIE, the annotations for subjects with expressions "disgust" at 0° and "neutral" at 15° are provided and we want to produce the annotations for subjects with expression "disgust" at 15°. In this case the annotated and non-annotated subsets are defined as $\mathcal{V} = \{Disgust, 0°, Neutral, 15°\}$ and $\mathcal{Q} = \{Disgust, 15°\}$, respectively.

In order to annotate the images in $\mathcal{Q}$, we first train an AOM using the images in $\mathcal{V}$. The trained model is employed within an iterative fitting procedure which

ACCEPTED MANUSCRIPT

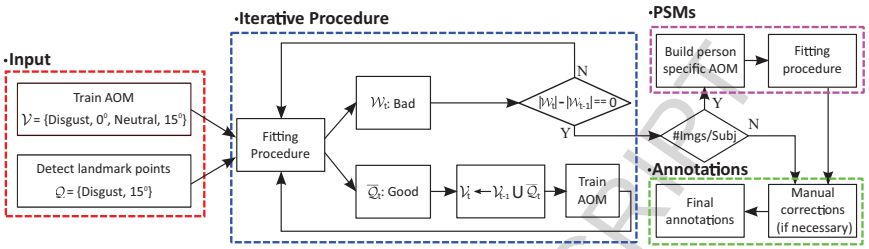

Figure 2: Flowchart of the proposed tool. Given a set of landmarked images $\mathcal{V}$ with various poses and expressions, we aim to annotate a set of non-annotated images $\mathcal{Q}$ (1) with the same subjects and different poses and expressions, or (2) with different subjects but similar pose and expressions.

aims to augment the set of correctly annotated images in $\mathcal{V}$ and build a more powerful AOM. Specifically, we fit the trained AOM to each image in $\mathcal{Q}$ and manually classify the fitting results into two sets: *Good* denoted as $\overline{\mathcal{Q}}$ and *Bad* denoted as $\mathcal{W} = \mathcal{Q} \setminus \overline{\mathcal{Q}}$. After this procedure is completed, the initial set of annotated images is augmented with $\overline{\mathcal{Q}}$, i.e. $\mathcal{V} \leftarrow \mathcal{V} \cup \overline{\mathcal{Q}}$, a new AOM is built using the updated $\mathcal{V}$ and the fitting procedure is repeated. This iterative process is repeated until the cardinality of the subset $\mathcal{W}$ has not changed between two consecutive iterations i.e., $|\mathcal{W}_t| - |\mathcal{W}_{t-1}| == 0$, thus we end up with fitting results for all the images in $\mathcal{Q}$. Note that we employ DPMs [17] to estimate the initial landmarks locations for the first iteration of the above procedure.

In case $\mathcal{Q}$ has multiple images per subject (e.g. Multi-PIE, XM2VTS, FRGC-V2, AR), the above method can be extended to further improve the generated annotations. Specifically, let us assume that we have a subset of images for each subject $\mathcal{Q}_p \subseteq \mathcal{Q}$ with N_p number of images each, where $p \in \{1, 2, \ldots, N_{subj}\}$. For each such subset, we build and fit a Person Specific Model (PSM) [39] in an "one-vs-rest" manner, that is we fit each image $\mathbf{i} \in \mathcal{Q}_p$ using the PSM trained on the rest $N_p - 1$ images. This person-specific adaptation further improves the results, especially since we employ person-specific AOMs. The generated annotations of the images in $\mathcal{Q}$ can be further manually improved, as a final step, although the above methodology ensures that minor corrections will be required. Figure 2 and Algorithm 1 present the flowchart and pseudocode, respectively, of the proposed semi-automatic annotation technique. Finally, the above method can be readily applied to annotate a database $\mathcal{DB}_1$ using an already annotated database $\mathcal{DB}_2$ by setting $\mathcal{V} = \mathcal{DB}_2$ and $\mathcal{Q} = \mathcal{DB}_1$.

3.3. Annotations

In this section, we present how the proposed tool was used in order to re-annotate the databases presented in Sec. 2. The advantages of the generated annotations[1] are twofold: (1) They all have the same landmarks configuration, i.e. the one employed in Multi-PIE (Fig. 1a), and (2) in many cases they are more accurate than the original ones.

ACCEPTED MANUSCRIPT

Algorithm 1 Semi-automatic database annotation tool

Require: Annotated subset $\mathcal{V}$, Non-annotated subset $\mathcal{Q}$
Ensure: Annotations of $\mathcal{Q}$
1: Initialize landmarks locations of $\mathcal{Q}$.
2: Initialize $\overline{\mathcal{Q}}_1 = \emptyset$, $\mathcal{V}_1 = \mathcal{V}$ and $\mathcal{W}_1 = \mathcal{Q}$.
3: $t = 1$.
4: **repeat**
5: Train an AOM using $\mathcal{V}_t$.
6: Fit the AOM to $\mathcal{W}_t$.
7: Manually classify the fittings to $\overline{\mathcal{Q}}_t$ (*Good*) and $\mathcal{W}_{t+1} = \mathcal{W}_t \setminus \overline{\mathcal{Q}}_t$ (*Bad*).
8: Update $\mathcal{V}_{t+1} \leftarrow \mathcal{V}_t \cup \overline{\mathcal{Q}}_t$.
9: $t \rightarrow t + 1$.
10: **until** $|\mathcal{W}_t| - |\mathcal{W}_{t-1}| == 0$
11: **if** multiple images per subject in $\mathcal{Q}$. **then**
12: **for** each subject $p = 1, 2, \ldots, N_{subj}$ **do**
13: $\mathcal{Q}_p \subseteq \mathcal{Q}$ is the subset with the N_p images of the subject.
14: **for** each image $\mathbf{i} \in \mathcal{Q}_p$ **do**
15: Train a person-specific AOM using $\mathcal{Q}_p \setminus \{\mathbf{i}\}$.
16: Fit the person-specific AOM to the image $\mathbf{i}$.
17: **end for**
18: **end for**
19: **end if**
20: Check and manually correct, if necessary, the generated annotations of $\mathcal{Q}$.

Multi-PIE: The available Multi-PIE annotations cover only the neutral expression with pose $[-45°, 45°]$ and multiple non-neutral expressions with pose $0°$. We employed the proposed tool to annotate 12570 images for 6 expressions, all 337 subjects and poses in range $[-30°, 30°]$.

XM2VTS: The images of XM2VTS's first session were semi-automatically annotated by setting $\mathcal{V}$ to be the subjects of Multi-PIE with neutral expression and $[-15°, 15°]$ poses. Subsequently, the annotated images of the first session were employed to annotate the images of the second session, and so on for all four available sessions. This procedure resulted in annotating 2360 images.

FRGC-V2: In the case of FRGC-V2, we first annotated a subset consisting of two images per subject with two different illumination conditions. This subset was annotated by employing images from Multi-PIE with six expressions and $[-15°, 15°]$ poses as $\mathcal{V}$. The rest of FRGC-V2 was annotated using this initial subset.

LFPW: Since LFPW database does not provide information regarding pose and expression characteristics for any image, we manually clustered the images in different poses $\{P_k\}$ in the range $[-30°, 30°]$. The images of each such pose cluster were semi-automatically annotated using images from Multi-PIE with the same pose.

HELEN, AFW, IBUG: The rest of in-the-wild databases were annotated

ACCEPTED MANUSCRIPT

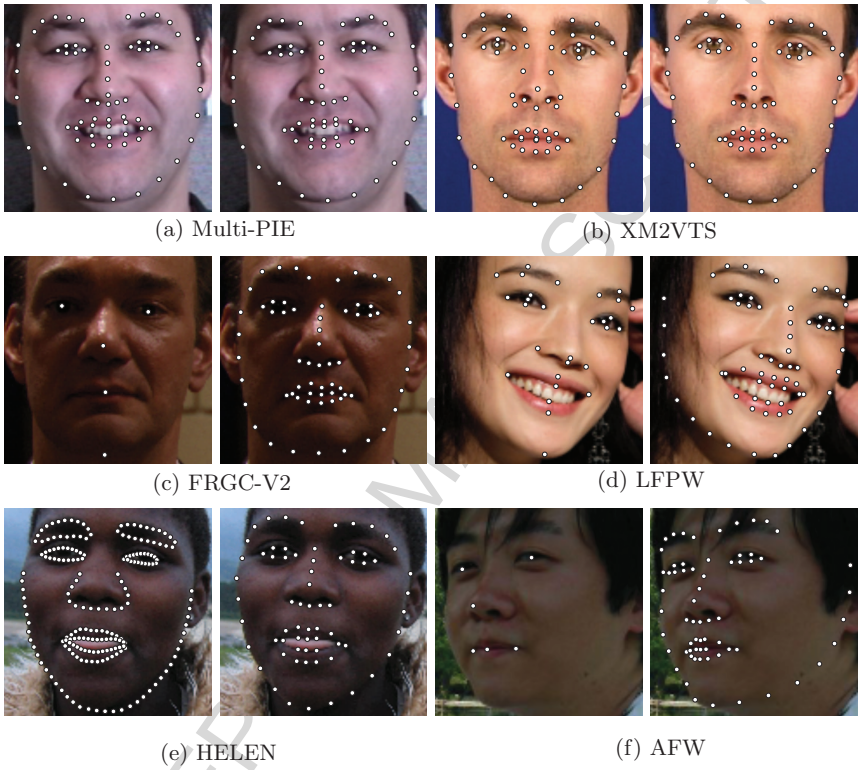

(a) Multi-PIE (b) XM2VTS

(c) FRGC-V2 (d) LFPW

(e) HELEN (f) AFW

Figure 3: Examples of the annotated images. For each database, the image on the *left* has the original annotations and the one on the *right* shows the annotations generated by the proposed tool. Note that in the case of Multi-PIE, even though the original and generated annotations have the same configuration, the generated ones are more accurate.

using a common procedure. Specifically, $\mathcal{Q}$ consisted of the non-annotated database $\mathcal{DB}_i$, and $\mathcal{V}$ was set equal to all the rest annotated in-the-wild databases $\mathcal{DB}_j,\ j = \{1, 2, \ldots, i-1\}$.

Figure 3 shows examples for each database with the original annotations and the annotations produced using the proposed semi-automatic methodology.

3.4. Efficiency

In order to assess the efficiency of the semi-automatic tool, we conducted the following experiment. We used the testing set of Helen database (330 images) as the annotated subset $\mathcal{V}$ while the non-annotated set $\mathcal{Q}$ was formed by randomly selecting 1450 images from the training set of the same database. Note that the selected images exhibit significant variations in pose, illumination and occlusion. Then, we applied the proposed semi-automatic tool in order to generate the annotations. Figure 4 visualizes the cardinality of $\mathcal{W}$ and $\mathcal{V}$ at each iteration until the termination of the procedure. The tool managed to generate

ACCEPTED MANUSCRIPT

annotations of good quality for 1393 out of 1450 images. The annotations for the rest 57 images were not adequately good mainly due to the existence of extreme poses, occlusions and illumination conditions. Given that an expert human annotator needs around 5 minutes to manually annotate from scratch one image, we have to spend 7250 minutes in order to annotate all the images. Instead, by using the proposed tool we dropped the requirement time for the creation of annotations in 1671 minutes. More specifically, we spent 820 minutes for the manual classification of fittings in *Good* and *Bad*, 549 minutes in order to refine the automatically created 1393 annotations, and 285 minutes for the manually annotation of the rest 57 images.

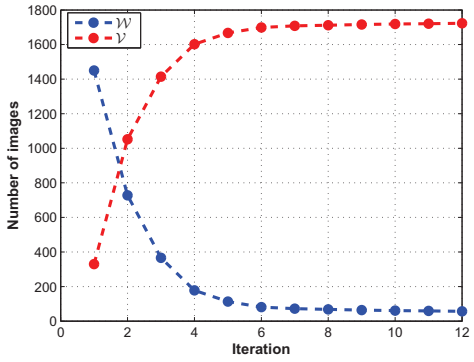

Figure 4: The cardinality of $\mathcal{W}$ and $\mathcal{V}$ per iteration.

3.5. Discussion

In order to assess the variance of the manually annotated landmarks, we considered the simplest case of annotating images with frontal faces without any occlusion or expression. To this end, we selected such images of $N = 80$ different subjects with frontal pose from the Multi-PIE database. All these images were manually annotated by three expert annotators. Figure 5 plots the variance of the manual annotations for each landmark point using an ellipse. Note that the ellipses are coloured based on the standard deviation of the annotations, normalized by the size of the face.

This experiment shows that the agreement level among the annotators is high for the landmarks that correspond to the eyes and mouth. This is due to the fact that these landmarks are located to facial features which are very distinctive across all human faces. Instead, the standard deviation is high for landmarks that do not have a clear semantic meaning. The chin is the most characteristic example of this category, as it demonstrates the highest variance. Finally, the result of this experiment suggests that it is more reliable to report the performance of landmark localization techniques using the 49-points mark-up (after removing the points of the face's boundary), as done in both 300W competitions.

ACCEPTED MANUSCRIPT

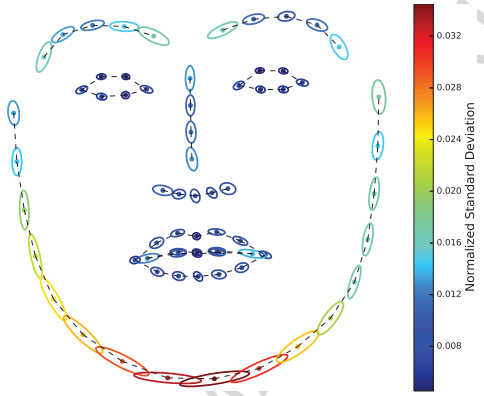

Figure 5: Each ellipse denotes the variance of each landmark point with regards to three expert human annotators. The colours of the points rank them with respect to their standard deviation normalized by the face size.

4. 300 Faces In-The-Wild Challenge

In this section, we present the 300 Faces In-The-Wild Challenge (300-W), the first facial landmark localization challenge that was held twice, in 2013 and 2015. The ultimate goal of the challenge is to provide a fair comparison between different automatic facial landmark detection methods. To this end, the 300-W database was collected and annotated using the same unified annotation scheme described in Sec. 3, in order to be used as testing set. Section 4.1 gives more details about the database and Sections 4.2 and 4.3 analyse the results of the two conducts of the competition.

4.1. 300-W Database

The 300-W database[4] is a newly-collected challenging dataset that consists of 300 *Indoor* and 300 *Outdoor* in-the-wild images. It covers a large variation of identity, expression, illumination conditions, pose, occlusion and face size. The images were downloaded from google.com by making queries such as "party", "conference", "protests", "football" and "celebrities". Compared to the rest of in-the-wild datasets, the 300-W database contains a larger percentage of partially-occluded images and covers more expressions than the common "neutral" or "smile", such as "surprise" or "scream". We annotated the images with the 68-points mark-up of Fig. 1a, using the semi-automatic methodology presented in Sec. 3. The images of the database were carefully selected so that they represent a characteristic sample of challenging but natural face instances under totally unconstrained conditions. Thus, methods that achieve accurate performance on the 300-W database can demonstrate the same accuracy in most realistic cases. Consequently, the experimental results on this database indicate how far the research community is from an adequately good solution to the problem of automatic facial landmarks localization.

ACCEPTED MANUSCRIPT

	Indoor	*Outdoor*
# faces	300	300
# images	222	177
Image size (range in pixels)	$[20.3k,\ 17.3M]$	$[27.2k,\ 21.0M]$
Face size (range in pixels)	$[5.0k,\ 0.8M]$	$[4.7k,\ 2.0M]$
Interoccular Distance (range in pixels)	$[42,\ 477]$	$[39,\ 805]$

Table 2: Overview of the characteristics of the 300-W database.

Table 2 summarizes the characteristics of the database. Many images of the database contain more than one annotated faces (293 images with 1 face, 53 images with 2 faces and 53 images with $[3, 7]$ faces). Consequently, the database consists of 600 annotated face instances, but 399 unique images. Finally, there is a large variety of face sizes. Specifically, 49.3% of the faces have size in the range $[48.6k,\ 2.0M]$ and the overall mean size is $85k$ (about 292×292) pixels.

4.2. 300-W Challenge: First Conduct (2013)

The first conduct of the 300-W challenge[2] was held in conjunction with IEEE International Conference on Computer Vision (ICCV) in 2013 [31].

Training. LFPW, AFW, HELEN, XM2VTS and FRGC-V2 were provided for training, along with the corrected annotations produced with the semi-automatic annotation tool (Sec 3). The fact that only a very small proportion of images in LFPW and HELEN have expressions different than "smile" motivated us to collect and annotate the IBUG database. It consists of 135 images with highly expressive faces under challenging poses and was provided to the participants as an additional option for training. Furthermore, we computed the bounding boxes of all the aforementioned databases by using our in-house face detector, the one that is also employed in [16], which is a variant of [17]. Both the annotations and the bounding boxes were made publicly available at the challenge's website[2]. Note that the participants were encouraged but not restricted to use only the provided training sets and annotations.

Testing. To ensure a fair comparison between the submitted methodologies, participants did not have access to the 300-W testing database. They were requested to send us the compiled (binary) files of their pre-trained systems. On our behalf, we extracted the face's bounding box for each of the testing images using the same methodology as the one employed for the training images[4]. These bounding boxes were passed in to the submitted executables as initializations. The accuracy of the fitting results was measured by the point-to-point RMS error between each fitted shape and the ground truth annotations, normalized by the face's interoccular distance, as proposed in [17]. Specifically, by denoting the fitted and ground truth shapes as $\mathbf{s}^f = [x_1^f, y_1^f, \ldots, x_N^f, y_N^f]^T$ and $\mathbf{s}^g =$

ACCEPTED MANUSCRIPT

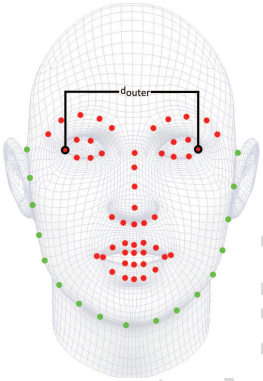

Figure 6: The 51-points mark-up is a subset of the 68-points one after removing the 17 points of the face's boundary. The interoccular distance is defined between the outer points of the eyes.

$[x_1^g, y_1^g, \ldots, x_N^g, y_N^g]^T$ respectively, then the error between them is computed as:

$$\text{RMSE} = \frac{\sum_{i=1}^{N} \sqrt{(x_i^f - x_i^g)^2 + (y_i^f - y_i^g)^2}}{d_{outer} N}, \tag{8}$$

where d_{outer} is the interoccular distance computed as the Euclidean distance between the outer points of each eye, as shown in Fig. 6. For the employed landmark configuration of Fig. 1a, the interoccular distance is defined as $d_{outer} = \sqrt{(x_{37}^g - x_{46}^g)^2 + (y_{37}^g - y_{46}^g)^2}$.

Participants. In total, there were six participants in this version of the challenge. Below is a brief description of the submitted methods:

- Baltrusaitis et al. [40] propose a probabilistic patch expert technique that learns non-linear and spatial relationships between the pixels and the probability of a landmark being aligned. To fit the model they propose a novel non-uniform regularised landmark mean-shift optimization technique which takes into account the reliabilities of each patch expert.
- Jaiswal et al. [41] use Local Evidence Aggregated Regression [42], in which local patches provide evidence of the location of the target facial point using Support Vector Regressors.
- Kamrul et al. [43] first apply a nearest neighbour search using global descriptors and, then, aim to align local neighbours by dynamically fitting a locally linear model to the global keypoint configurations of the returned neighbours. Neighbours are also used to define restricted areas of the input image in which they apply local discriminative classifiers. Finally, an energy minimization approach is applied in order to combine the local classifier predictions with the dynamically estimated joint keypoint configuration model.

ACCEPTED MANUSCRIPT

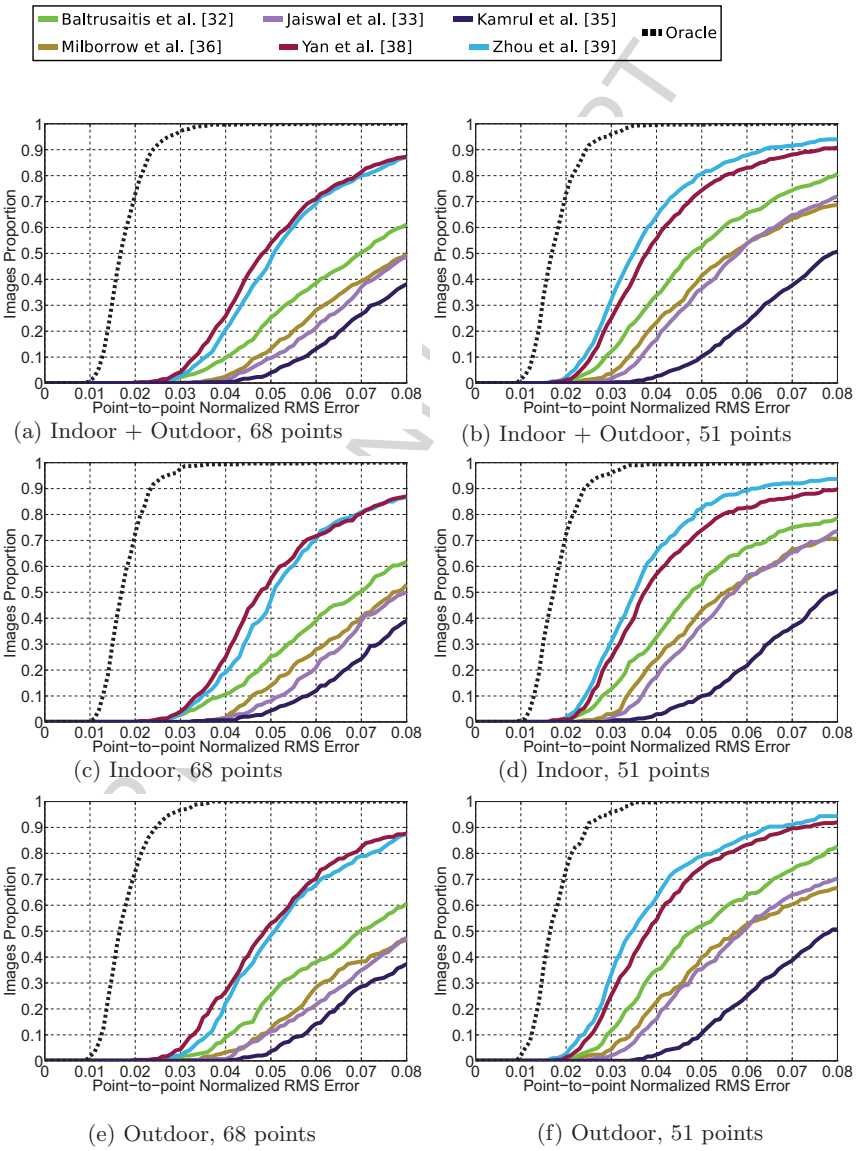

(a) Indoor + Outdoor, 68 points

(b) Indoor + Outdoor, 51 points

(c) Indoor, 68 points

(d) Indoor, 51 points

(e) Outdoor, 68 points

(f) Outdoor, 51 points

Figure 7: Fitting results of the *first* conduct of the 300-W challenge in *2013*. The plots show the Cumulative Error Distribution (CED) curves with respect to the landmarks (68 and 51 points) and the condtions (indoor, outdoor or both).

- Milborrow et al. [44] approach the problem with Active Shape Models (ASMs) that incorporate a modified version of SIFT descriptors [45]. They employ multiple ASMs and utilize the one that best estimates the face's yaw pose.

ACCEPTED MANUSCRIPT

Participant	*68 points*	*51 points*
Baltrusaitis et al. [40]	0.0486	0.0388
Jaiswal et al. [41]	0.0527	0.0506
Kamrul et al. [43]	0.0543	0.0551
Milborrow et al. [44]	0.1126	0.1145
Yan et al. [46]	0.0211	0.0199
Zhou et al. [47]	0.0205	0.0182
Oracle	0.0038	0.0040

Table 3: Median absolute deviation of the fitting results of the *first* conduct of 300-W challenge in *2013*, reported for both 68 and 51 points.

- Yan et al. [46] employ a cascade regression framework, where a series of regressors are utilized to progressively refine the shape initialized by the face detector. In order to handle inaccurate initializations from the face detector, they generate multiple hypotheses and learn to rank or combine them in order to get the final results. They estimate the parameters in both "learn to rank" and "learn to combine" using a structural Support Vector Machine framework.

- Zhou et al. [47] propose a four-level convolutional network cascade, where each level is trained to locally refine the outputs of the previous network levels. Moreover, each level predicts an explicit geometric constraint (face region and component position) to rectify the inputs of the next levels, which improves the accuracy and robustness of the whole network structure.

Results. The performance of the submitted systems was assessed based on both the 68 and 51 points. As shown in Fig. 6, the 51 points are a subset of the 68 points after removing the 17 points of the face's boundary. Figure 7 shows the Cumulative Error Distribution (CED) curves using the error metric of Eq. 8. The plots are divided based on the number of points (68 and 51) as well as the images subsets (*Indoor*, *Outdoor* and *Indoor* + *Outdoor*). Table 3 reports the median absolute deviation of the results and Fig. 10 shows some indicative fitting shapes.

All methodologies demonstrated a lower performance on *Outdoor* scenes. The main reason for this is the illumination variance which is much smaller within an *Indoor* environment. However, another factor affecting the performance is that the *Outdoor* images have larger variation in facial expressions compared to the *Indoor* ones. This is because we picked specific keywords for the selection of *Outdoor* images, such as "sports" and "protest", which ended up in a big number of images with various expressions, such as "surprise" and "scream", that are much more challenging than the expressions that are commonly seen in the *Indoor* ones, such as "smile" and "neutral". We decided to announce two winners: one from an academic institution and one from industry.

ACCEPTED MANUSCRIPT

	Indoor	*Outdoor*
# faces	300	300
# images	300	300
Image size (range in pixels)	$[16.2k,\ 3.3M]$	$[11.2k,\ 4.5M]$
Face size (range in pixels)	$[5.0k,\ 0.8M]$	$[4.7k,\ 2.0M]$
Interoccular Distance (range in pixels)	$[42,\ 477]$	$[39,\ 805]$

Table 4: Overview of the characteristics of the cropped images of the 300-W database.

Based on the results, the winners were (a) Yan et al. [46] from The National Laboratory of Pattern Recognition at the Institute of Automation of the Chinese Academy of Sciences, and (b) Zhou et al. [47] from Megvii company. It is worth to mention that all groups achieved better results in the case of 51 points.

In order to show whether there is any room for further improvement on the performance, we also report an Oracle curve. We built a statistical shape model using the shapes of the training databases, as explained in Eq. 1, and kept the first 25 components. Using this model, we compute and plot the reconstruction error for each shape of the 300-W database. The reconstruction of a shape $\mathbf{s}$ is achieved by first projecting as $\mathbf{p}_r = \mathbf{U}^T(\mathbf{s} - \bar{\mathbf{s}})$, and then reconstructing as $\mathbf{s}_r = \bar{\mathbf{s}} + \mathbf{U}\mathbf{p}_r$. The resulting curve shows that the 300-W dataset is not saturated and there is considerable room for further improvement.

4.3. 300-W Challenge: Second Conduct (2015)

The second conduct of the 300-W challenge was completed in the beginning of 2015. The biggest difference compared to the previous conduct is that we were no longer providing the bounding boxes of the images to the fitting methods. On the contrary, the participants were required to submit systems that perform both face detection and landmark localization. The three main reasons that led us to this change are:

1. Various techniques perform differently when initialized with bounding boxes that cover different facial region. For example, DPMs [17] tend to return bounding boxes that only include facial texture and not any of the subject's hair, as usually done by the Viola-Jones detector [48].
2. There are methods, like DPMs [17] and Pictorial Structures [11, 12], that do not require any initialization.
3. There are algorithms for which the training is coupled with the face detector, such as SDM [18].

Of course, this change made the task even more challenging than before, since the search region of each image became much larger with a lot of background information.

300-W Images Cropping. As mentioned in Sec. 4.1, many of the 300-W images contain more than one faces, which are not necessarily annotated. Consequently, we cropped the images so that they all included only *one* face. The cropping

ACCEPTED MANUSCRIPT

Figure 8: Indicative examples of the way the images were cropped for the second conduct of the 300-W challenge.

was performed in such a way to ensure that (1) only a single face is included in each image and (2) DPMs [17] and Viola-Jones [48] achieve the best true positive rate that they possibly can. Table 4 reports the characteristics of the cropped images. Naturally, the only thing that changes compared to the ones of the initial images in Tab. 2 is the image size (resolution). The mean size of the cropped images is $0.4M$ pixels, which is much smaller than the $3.3M$ pixels of the non-cropped images. Figure 8 shows some representative examples of the way that the images were cropped. Note that the cropped images are provided along with the original images of the 300-W database[4].

Training. The training instructions were the same as in the previous conduct. The authors were encouraged, but not restricted, to use LFPW, AFW, HELEN, IBUG, FRGC-V2 and XM2VTS databases with the provided annotations.

Testing. The testing procedure followed the same rules as in the previous version of the challenge. The participants were required to submit compiled pre-trained systems, the performance of which was evaluated using the metric of Eq. 8. The submitted systems could return nothing in case no face was detected or the detected face was estimated to be a false positive. Consequently, in order to facilitate the participants and make the competition less dependent to a face

ACCEPTED MANUSCRIPT

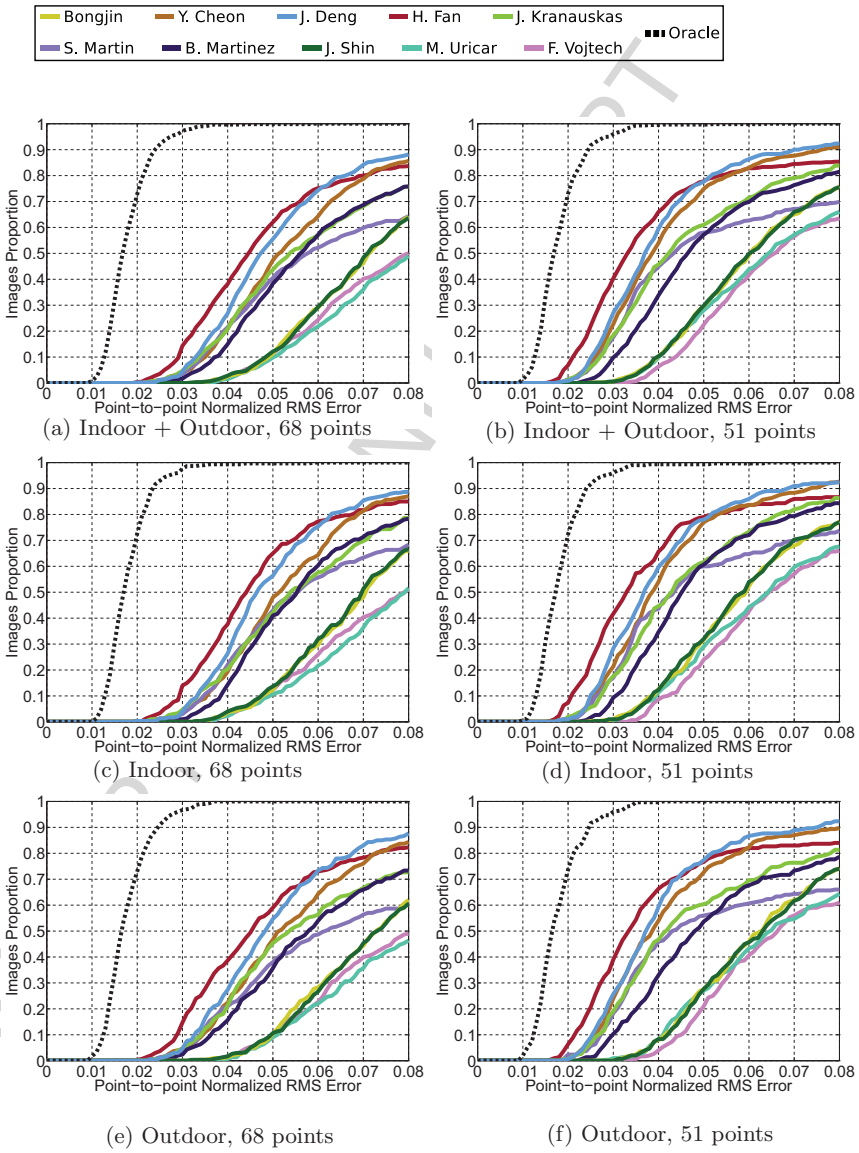

(a) Indoor + Outdoor, 68 points

(b) Indoor + Outdoor, 51 points

(c) Indoor, 68 points

(d) Indoor, 51 points

(e) Outdoor, 68 points

(f) Outdoor, 51 points

Figure 9: Fitting results of the *second* conduct of the 300-W challenge in *2015*. The plots show the Cumulative Error Distribution (CED) curves with respect to the landmarks (68 and 51 points) and the condtions (indoor, outdoor or both).

detector's performance, we suggested them to use one of the face detection methods that took part in the Face Detection Data Set and Benchmark (FDDB) [49]. Finally, in this conduct of the competition, the submitted methods were also assessed with respect to their computational costs and a maximum limit of 2 minutes per image was typically set.

ACCEPTED MANUSCRIPT

Participant	*# images with detection*	*mad*		*timings (secs)*
		68 points	*51 points*	
Bongjin	584 (97.3%)	0.0271	0.0249	12.9
Y. Cheon	600 (100%)	0.1078	0.1040	0.17
J. Deng	599 (99.8%)	0.0226	0.0213	1.97
H. Fan	526 (87.7%)	0.0309	0.0294	1.29
J. Kranauskas	600 (100%)	0.0693	0.0659	2.46
S. Martin	597 (99.5%)	0.3461	0.3228	5.81
B. Martinez	600 (100%)	0.0514	0.0497	42.5
J. Shin	585 (97.5%)	0.0303	0.0287	12.6
M. Uricar	592 (98.7%)	0.0970	0.0945	3.46
F. Vojtech	591 (98.5%)	0.1047	0.0998	4.05
Oracle	–	0.0038	0.0040	–

Table 5: Second conduct of the 300-W challenge. *2nd column:* Number of images for which an estimation of the landmarks was returned. *3rd and 4th columns:* The mean absolute deviation of the fitting results for both 68 and 51 points. *5th column:* Mean computational cost per method.

Results. The number of participants in this version of the competition was 10. Figure 9 shows the CED curves of the submitted methodologies. Table 5 reports the number of images for which an estimation of the landmarks was returned, the mean absolute deviation of the results, as well as the mean computational costs. The common subset of images for which all methods returned a detection consists of 517 images. Figure 11 shows some indicative fitting results.

Based on the results, the winner of the competition is J. Deng with small difference from the second best performing method of H. Fan. Even though the technique of H. Fan is slightly more accurate, it returns results 526 images, as opposed to the one of J. Deng that detects the landmarks in 599 images and has a small mean absolute deviation. It is worth to notice that some systems employed an unreliable face detector. This seems to be the case with S. Martin. Their system returned an output for 597 images and, even though most of them have an adequately accurate result, there is a percentage of about 26% of images for which the error is very high because of false positive face detections. This is the reason why their mean absolute deviation is high. Moreover, only three submissions managed to return a detection for all 600 images: Y. Cheon, J. Kranauskas and B. Martinez. The results indicate that especially in the case of J. Kranauskas and B. Martinez, even though their methodologies are not the most accurate ones, they are though very robust with small mean absolute deviations. Finally, the system of J. Deng is also the third fastest one behind Y. Cheon and H. Fan. It is worth to note that Y. Cheon technique is much faster than the rest of the submissions (170 milliseconds per image) while achieving quite accurate results.

ACCEPTED MANUSCRIPT

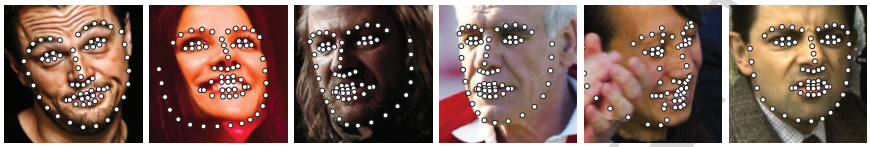

(a) Baltrusaitis et al. [40]

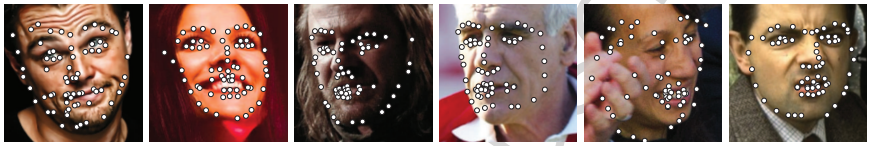

(b) Jaiswal et al. [41]

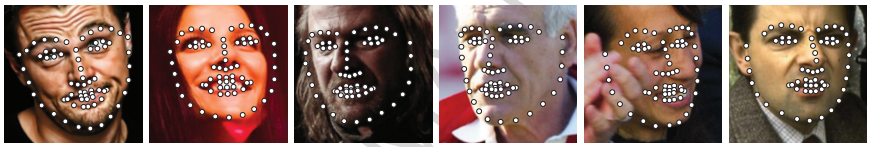

(c) Kamrul et al. [43]

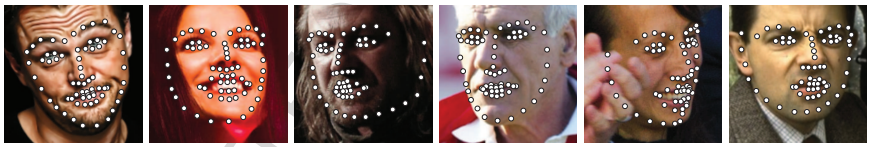

(d) Milborrow et al. [44]

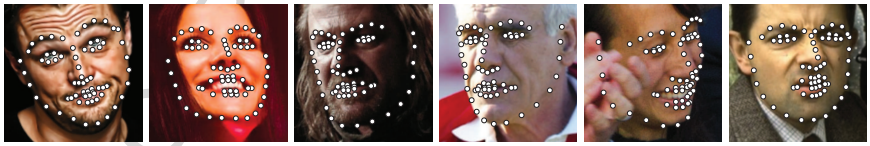

(e) Yan et al. [46]

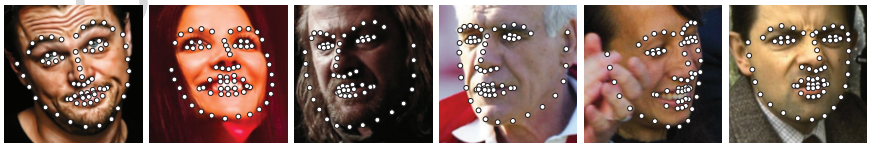

(f) Zhou et al. [47]

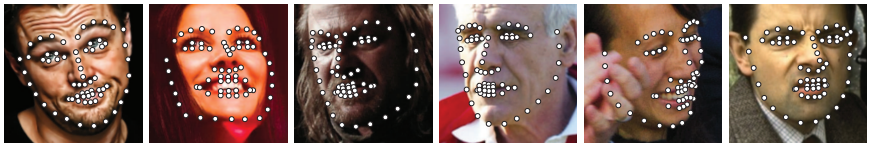

(g) Ground truth

Figure 10: Fitting examples of the *first* conduct of the 300-W challenge in *2013*. Each row shows the fitted landmarks for each participating method.

ACCEPTED MANUSCRIPT

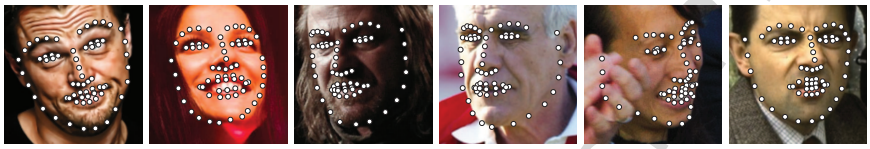

(a) Bongjin

(b) Y. Cheon

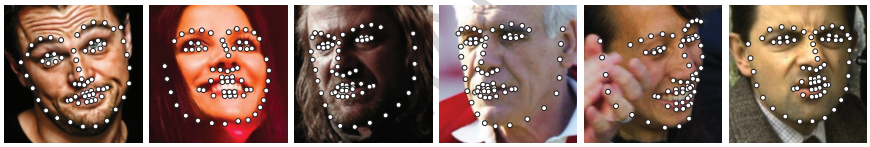

(c) J. Deng

(d) H. Fan

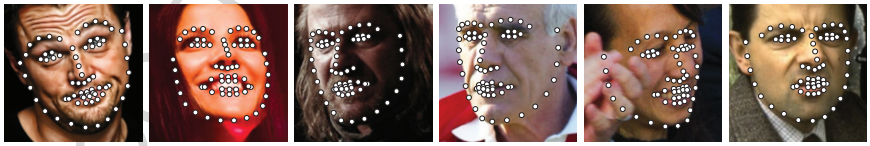

(e) J. Kranauskas

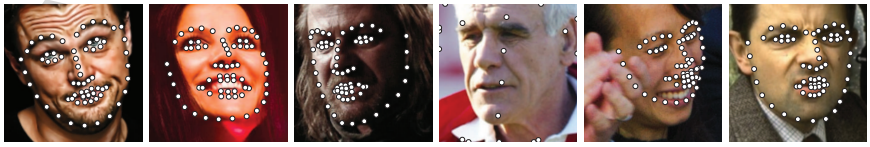

(f) S. Martin

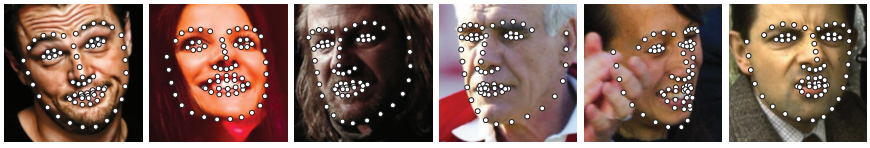

(g) B. Martinez

ACCEPTED MANUSCRIPT

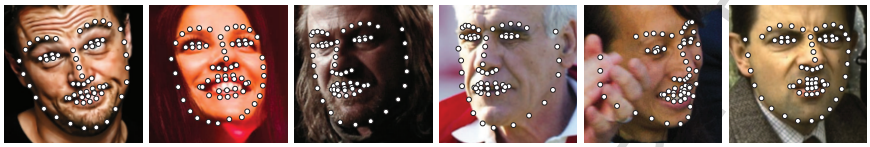

(h) J. Shin

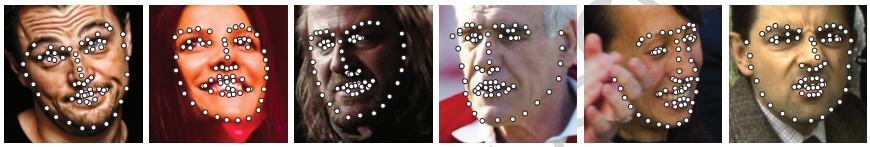

(i) M. Uricar

(j) F. Vojtech

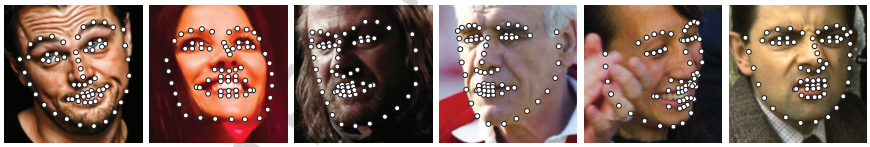

(k) Ground truth

Figure 11: Fitting examples of the *second* conduct of the 300-W challenge in *2015*. Each row shows the fitted landmarks for each participating method.

5. Discussion and Conclusions

The results of both conducts of the 300-W challenge shown in Figs. 7 and 9 clearly prove that, even though much progress has been made during the last years, the research community is still far from accurately solving the problem of face alignment and that there is much room for further improvement. This is indicated by the gap between the participants' curves and the Oracle, which is the minimum error that can be achieved using the specific training databases. Table 6 reports the percentage of images with error less than $\{0.02, 0.03, 0.04, 0.05, 0.06\}$ for the top techniques of both competitions as well as the Oracle and makes it obvious that the gap is still huge, especially for small error values.

Table 6 also shows that there was a small improvement on the state-of-the-art performance between the first and the second conduct of the challenge. The top performing methodologies have relatively small differences and are close to each other. One of the main reasons behind this progress is the plethora of training data from which discriminative methods can greatly benefit. For example, techniques like Yan et al. [46] (cascade regression framework) and

ACCEPTED MANUSCRIPT

Method	< 0.02	< 0.03	< 0.04	< 0.05	< 0.06
Yan et al. [46]	0.17%	4.17%	25.8%	54.0%	71.0%
Zhou et al. [47]	0%	2.50%	20.7%	47.7%	69.2%
J. Deng	0.17%	4.33%	26.8%	55.5%	74.3%
H. Fan	0.33%	14.3%	38.2%	62.0%	75.2%
Oracle	72.8%	97.2%	99.7%	99.8%	100%

Table 6: Percentage of images with fitting error less than the specified values for the winners of the first (Yan et al. [46], Zhou et al. [47]) and second (J. Deng, H. Fan) 300-W challenges, and Oracle. The error is based on 68 points using both indoor and oudoor images.

Zhou et al. [47] (convolutional network framework), can continually achieve better results with continuous rise in the amount of training data.

Additionally, the 300-W challenge was only focused on the task of *sparse* facial landmark points detection. Alignment using dense landmark mark-ups is much more difficult and the performance would get worse. This is because the more landmarks exist in the shape, there is more ambiguity about the semantic locations at which they are located. Consider for example the 41 boundary landmark points of the HELEN mark-up in Fig. 1f. Their locations have no special semantic discrimination. On the contrary they are just located with an approximately equal distance between them. Consequently, it is very hard to accurate detect such points since there is no discriminative texture information that describes them and which could drive the fitting procedure. This highlights the need to further research how to select a relatively high number of landmark points that are capable to describe all the characteristic areas of an object.

Moreover, another factor that contributed towards creating more accurate and efficient alignment techniques is the great progress in the task of face detection. Most landmark localization methodologies are very sensitive to the initialization, thus the face detection performance. The results presented in the Face Detection Data Set and Benchmark (FDDB) [49] show that current state-of-the-art techniques achieve very good true positive rates. However, there is still room for further improvement especially on images with in-the-wild conditions.

Finally, most current research effort focuses on detecting the facial landmarks and not tracking them within video sequences. We strongly believe that more attention should be given towards developing techniques that can track facial points in a robust manner, even under difficult conditions such as camera movement, disappearance and re-appearance of the face, challenging background and lighting, etc. Consequently, we believe that one promising step towards this direction would be the organization of a challenge, similar to the 300-W one, that focuses on facial landmark points tracking. The biggest difficulty of such a competition would be the annotation of the thousands of frames of the videos. However, using semi-automatic annotation tools as the one proposed in this paper, the task would be simplified and annotations could be efficiently generated.

ACCEPTED MANUSCRIPT

6. Acknowledgments

This work is funded by the EPSRC project EP/J017787/1 (4D-FAB). The work by S. Zafeiriou is also partially supported by the EPSRC project EP/L026813/1 Adaptive Facial Deformable Models for Tracking (ADAManT). The work by M. Pantic is further supported by the European Community Horizon 2020 [H2020/2014-2020] under grant agreement no. 645094 (SEWA). The work of G. Tzimiropoulos is also partially supported by EPSRC project EP/M02153X/1 Facial Deformable Models of Animals.

[1] T. F. Cootes, G. J. Edwards, C. J. Taylor, Active appearance models, IEEE Transactions on Pattern Analysis and Machine Intelligence 23 (6) (2001) 681–685.

[2] I. Matthews, S. Baker, Active appearance models revisited, International Journal of Computer Vision 60 (2) (2004) 135–164.

[3] G. Tzimiropoulos, J. Alabort-i-Medina, S. Zafeiriou, M. Pantic, Generic active appearance models revisited, in: Proceedings of Asian Conference on Computer Vision (ACCV), Daejeon, Korea, 2012, pp. 650–663.

[4] G. Tzimiropoulos, J. Alabort-i-Medina, S. Zafeiriou, M. Pantic, Active orientation models for face alignment in-the-wild, IEEE Transactions on Information Forensics and Security, Special Issue on Facial Biometrics in-the-wild 9 (2014) 2024–2034.

[5] G. Tzimiropoulos, M. Pantic, Optimization problems for fast aam fitting in-the-wild, in: Proceedings of IEEE International Conference on Computer Vision (ICCV), 2013.

[6] E. Antonakos, J. Alabort-i-Medina, G. Tzimiropoulos, S. Zafeiriou, Hog active appearance models, in: Proceedings of IEEE International Conference on Image Processing (ICIP), Paris, France, 2014, pp. 224–228.

[7] J. Alabort-i-Medina, S. Zafeiriou, Bayesian active appearance models, in: Proceedings of IEEE International Conference on Computer Vision & Pattern Recognition (CVPR), 2014.

[8] J. Alabort-i Medina, S. Zafeiriou, Unifying holistic and parts-based deformable model fitting, in: Proceedings of IEEE International Conference on Computer Vision & Pattern Recognition (CVPR), 2015, pp. 3679–3688.

[9] G. Tzimiropoulos, M. Pantic, Gauss-newton deformable part models for face alignment in-the-wild, in: Proceedings of IEEE International Conference on Computer Vision & Pattern Recognition (CVPR), IEEE, 2014, pp. 1851–1858.

[10] E. Antonakos, J. Alabort-i Medina, S. Zafeiriou, Active pictorial structures, in: Proceedings of IEEE International Conference on Computer Vision & Pattern Recognition (CVPR), 2015, pp. 5435–5444.

ACCEPTED MANUSCRIPT

[11] P. F. Felzenszwalb, D. P. Huttenlocher, Pictorial structures for object recognition, International Journal of Computer Vision 61 (1) (2005) 55–79.

[12] M. Andriluka, S. Roth, B. Schiele, Pictorial structures revisited: People detection and articulated pose estimation, in: Proceedings of IEEE International Conference on Computer Vision & Pattern Recognition (CVPR), IEEE, 2009, pp. 1014–1021.

[13] T. F. Cootes, C. J. Taylor, D. H. Cooper, J. Graham, Active shape models-their training and application, Computer Vision and Image Understanding 61 (1) (1995) 38–59.

[14] D. Cristinacce, T. Cootes, Feature detection and tracking with constrained local models, in: Proceedings of British Machine Vision Conference (BMVC), Vol. 3, 2006, pp. 929–938.

[15] J. M. Saragih, S. Lucey, J. F. Cohn, Deformable model fitting by regularized landmark mean-shift, International Journal of Computer Vision 91 (2) (2011) 200–215.

[16] A. Asthana, S. Zafeiriou, S. Cheng, M. Pantic, Robust discriminative response map fitting with constrained local models, in: Proceedings of IEEE International Conference on Computer Vision & Pattern Recognition (CVPR), IEEE, 2013, pp. 3444–3451.

[17] X. Zhu, D. Ramanan, Face detection, pose estimation, and landmark localization in the wild, in: Proceedings of IEEE International Conference on Computer Vision & Pattern Recognition (CVPR), IEEE, 2012, pp. 2879–2886.

[18] X. Xiong, F. De la Torre, Supervised descent method and its applications to face alignment, in: Proceedings of IEEE International Conference on Computer Vision & Pattern Recognition (CVPR), IEEE, 2013, pp. 532–539.

[19] X. Cao, Y. Wei, F. Wen, J. Sun, Face alignment by explicit shape regression, International Journal of Computer Vision 107 (2) (2014) 177–190.

[20] A. Asthana, S. Zafeiriou, S. Cheng, M. Pantic, Incremental face alignment in the wild, in: Proceedings of IEEE International Conference on Computer Vision & Pattern Recognition (CVPR), IEEE, 2014, pp. 1859–1866.

[21] G. Tzimiropoulos, Project-out cascaded regression with an application to face alignment, in: Proceedings of IEEE International Conference on Computer Vision & Pattern Recognition (CVPR), IEEE, 2015, pp. 3659–3667.

[22] S. Ren, X. Cao, Y. Wei, J. Sun, Face alignment at 3000 fps via regressing local binary features, in: Proceedings of IEEE International Conference on Computer Vision & Pattern Recognition (CVPR), IEEE, 2014, pp. 1685–1692.

ACCEPTED MANUSCRIPT

[23] V. Kazemi, J. Sullivan, One millisecond face alignment with an ensemble of regression trees, in: Proceedings of IEEE International Conference on Computer Vision & Pattern Recognition (CVPR), IEEE, 2014, pp. 1867–1874.

[24] R. Gross, I. Matthews, J. Cohn, T. Kanade, S. Baker, Multi-pie, Image and Vision Computing 28 (5) (2010) 807–813.

[25] K. Messer, J. Matas, J. Kittler, J. Luettin, G. Maitre, Xm2vtsdb: The extended m2vts database, in: Second international conference on audio and video-based biometric person authentication, Vol. 964, Citeseer, 1999, pp. 965–966.

[26] P. Phillips, P. Flynn, T. Scruggs, K. Bowyer, J. Chang, K. Hoffman, J. Marques, J. Min, W. Worek, Overview of the face recognition grand challenge, in: Proceedings of IEEE International Conference on Computer Vision & Pattern Recognition (CVPR), IEEE, 2005, pp. 947–954.

[27] A. M. Martinez, The ar face database, CVC Technical Report 24.

[28] P. N. Belhumeur, D. W. Jacobs, D. Kriegman, N. Kumar, Localizing parts of faces using a consensus of exemplars, in: Proceedings of IEEE International Conference on Computer Vision & Pattern Recognition (CVPR), IEEE, 2011, pp. 545–552.

[29] V. Le, J. Brandt, Z. Lin, L. Bourdev, T. S. Huang, Interactive facial feature localization, in: Proceedings of European Conference on Computer Vision (ECCV), Springer, 2012, pp. 679–692.

[30] M. Kostinger, P. Wohlhart, P. M. Roth, H. Bischof, Annotated facial landmarks in the wild: A large-scale, real-world database for facial landmark localization, in: Proceedings of IEEE International Conference on Computer Vision (ICCV-W), Workshop on Benchmarking Facial Image Analysis Technologies, IEEE, 2011, pp. 2144–2151.

[31] C. Sagonas, G. Tzimiropoulos, S. Zafeiriou, M. Pantic, 300 faces in-the-wild challenge: The first facial landmark localization challenge, in: Proceedings of IEEE International Conference on Computer Vision (ICCV-W), Workshop on 300 Faces in-the-Wild Challenge (300-W), Sydney, Australia, 2013.

[32] J. Alabort-i-Medina, E. Antonakos, J. Booth, P. Snape, S. Zafeiriou, Menpo: A comprehensive platform for parametric image alignment and visual deformable models, in: Proceedings of the ACM International Conference on Multimedia, Open Source Software Competition, Orlando, FL, USA, 2014, pp. 679–682.

[33] X. Jia, H. Yang, A. Lin, K.-P. Chan, I. Patras, Structured semi-supervised forest for facial landmarks localization with face mask reasoning, in: Proceedings of British Machine Vision Conference (BMVC), 2014.

ACCEPTED MANUSCRIPT

[34] M. Pedersoli, T. Tuytelaars, L. V. Gool, Using a deformation field model for localizing faces and facial points under weak supervision, in: Proceedings of IEEE International Conference on Computer Vision & Pattern Recognition (CVPR), 2014, pp. 3694–3701.

[35] Y. Tong, X. Liu, F. W. Wheeler, P. H. Tu, Semi-supervised facial landmark annotation, Computer Vision and Image Understanding 116 (8) (2012) 922–935.

[36] Y. Wu, Z. Wang, Q. Ji, A hierarchical probabilistic model for facial feature detection, in: Proceedings of IEEE International Conference on Computer Vision & Pattern Recognition (CVPR), 2014, pp. 1781–1788.

[37] G. Tzimiropoulos, S. Zafeiriou, M. Pantic, Subspace learning from image gradient orientations, IEEE Transactions on Pattern Analysis and Machine Intelligence 34 (12) (2012) 2454–2466.

[38] G. Papandreou, P. Maragos, Adaptive and constrained algorithms for inverse compositional active appearance model fitting, in: Proceedings of IEEE International Conference on Computer Vision & Pattern Recognition (CVPR), IEEE, 2008, pp. 1–8.

[39] R. Gross, I. Matthews, S. Baker, Generic vs. person specific active appearance models, Image and Vision Computing 23 (12) (2005) 1080–1093.

[40] T. Baltrusaitis, P. Robinson, L.-P. Morency, Constrained local neural fields for robust facial landmark detection in the wild, in: Proceedings of IEEE International Conference on Computer Vision (ICCV-W), Workshop on 300 Faces in-the-Wild Challenge (300-W), 2013, pp. 354–361.

[41] S. Jaiswal, T. Almaev, M. Valstar, Guided unsupervised learning of mode specific models for facial point detection in the wild, in: Proceedings of IEEE International Conference on Computer Vision (ICCV-W), Workshop on 300 Faces in-the-Wild Challenge (300-W), 2013, pp. 370–377.

[42] B. Martinez, M. F. Valstar, X. Binefa, M. Pantic, Local evidence aggregation for regression-based facial point detection, IEEE Transactions on Pattern Analysis and Machine Intelligence 35 (5) (2013) 1149–1163.

[43] M. Hasan, C. Pal, S. Moalem, Localizing facial keypoints with global descriptor search, neighbour alignment and locally linear models, in: Proceedings of IEEE International Conference on Computer Vision (ICCV-W), Workshop on 300 Faces in-the-Wild Challenge (300-W), 2013, pp. 362–369.

[44] S. Milborrow, T. Bishop, F. Nicolls, Multiview active shape models with sift descriptors for the 300-w face landmark challenge, in: Proceedings of IEEE International Conference on Computer Vision (ICCV-W), Workshop on 300 Faces in-the-Wild Challenge (300-W), 2013, pp. 378–385.

ACCEPTED MANUSCRIPT

[45] D. G. Lowe, Object recognition from local scale-invariant features, in: Proceedings of IEEE International Conference on Computer Vision (ICCV), Vol. 2, IEEE, 1999, pp. 1150–1157.

[46] J. Yan, Z. Lei, D. Yi, S. Li, Learn to combine multiple hypotheses for accurate face alignment, in: Proceedings of IEEE International Conference on Computer Vision (ICCV-W), Workshop on 300 Faces in-the-Wild Challenge (300-W), 2013, pp. 392–396.

[47] E. Zhou, H. Fan, Z. Cao, Y. Jiang, Q. Yin, Extensive facial landmark localization with coarse-to-fine convolutional network cascade, in: Proceedings of IEEE International Conference on Computer Vision (ICCV-W), Workshop on 300 Faces in-the-Wild Challenge (300-W), 2013, pp. 386–391.

[48] P. Viola, M. Jones, Rapid object detection using a boosted cascade of simple features, in: Proceedings of IEEE International Conference on Computer Vision & Pattern Recognition (CVPR), IEEE, 2001.

[49] V. Jain, E. Learned-Miller, Fddb: A benchmark for face detection in unconstrained settings, Tech. Rep. UM-CS-2010-009, University of Massachusetts, Amherst (2010).

ACCEPTED MANUSCRIPT

ACCEPTED MANUSCRIPT

Highlights

- We propose a semi-automatic methodology for facial landmark points annotation.
- We present and analyse the results of the 300 Faces In-The-Wild Challenge.
- We make the challenging 300-W dataset publicly available to the research community.

ACCEPTED MANUSCRIPT